

SELF-CONSISTENT EQUILIBRIA OF ACCELERATED  
RELATIVISTIC ELECTRON RINGS

I. Hofmann

Max Planck-Institut für Plasmaphysik<sup>+</sup>  
Garching bei München/BRD

Summary

A self-consistent model and numerical code for a relativistic electron ring loaded with ions was developed, using realistic distribution functions for adiabatically changing equilibria. The main result is that in an ion-focussed ring the "holding power"  $eE_R$  is only about 20% of the ring peak electric field, whereas an additional electric image cylinder ("squirrel cage") allows ion acceleration up to 80% of the peak electric field.

A. Introduction

Collective ion acceleration by the strong electric fields in a ring of relativistic electrons has been the subject of many investigations in the past few years.

In order to establish performance characteristics for an electron ring accelerator (ERA), one has to consider instability problems as well as the equilibrium state. Instabilities turned out to impose severe limits on the effectiveness of ion acceleration<sup>1</sup>. The study of equilibrium is not only the starting point for instability investigations, but is also necessary for the basic question of the "holding power", which will be treated in this paper. Equilibrium models have been used in the past which often showed a substantial lack of self-consistency from the point of view of the Vlasov equation. Most of the theoretical work has been done along the following lines:

1. self-consistent particle codes<sup>1</sup>; with present-day computers they are restricted to short physical times and thus inappropriate for adiabatically changing equilibria.

2. virial theorems and macroscopic fluid models<sup>2,3,4</sup>.

3. models based on the Vlasov equation; simple models for rings at rest use uniform densities and harmonic betatron oscillations<sup>5,6,7</sup> while others study nonuniform density effects without being self-consistent<sup>8,9</sup>, or calculate realistic ion distribution functions for uniform electron density<sup>10</sup>, whereas accelerated equilibria are treated numerically employing microcanonical distribution functions and approximating ring cross-sections by ellipses<sup>11</sup>.

The present paper is free from the simplifications of the above-mentioned models and gives numerical solutions of accelerated ring equilibria that are self-consistent within the framework of the Vlasov-Maxwell equations. In particular, it uses physically relevant distribution functions for either particle species and takes into account their time-dependence by means of appropriate adiabatic invariants.

B. Stationary Vlasov Equilibria  
for an Electron Ring with Ions

I. Basic Equations

For axisymmetric fields the electron motion is governed by the relativistic Hamiltonian in cylindrical coordinates

$$H_e = (m_e c^4 + e^2 p^2)^{1/2} - e \phi(r, z), \quad \frac{\partial H_e}{\partial \theta} = 0$$

$$p = \{p_r, p_\theta, p_z\}, \quad p_r = \frac{p}{r} + \frac{e}{c} A_\theta(r, z), \quad \dot{p}_\theta = 0 \quad \text{with (1)}$$

$$\text{and particle velocities } v = \frac{p}{m_e \gamma}, \quad \gamma^2 = (1 - v^2)^{-1}$$

$A_\theta$  is the only non-vanishing component of the vector potential and  $\phi$  the scalar potential, including self-fields  $A_\theta = A_\theta^{\text{ext}} + A_\theta^{\text{int}}$ ,  $\phi = \phi^{\text{ext}}$

Ion motion is prescribed by the nonrelativistic Hamiltonian

$$H_i = \frac{p^2}{2m_i} + e\phi(r, z) \quad (2)$$

where magnetic field effects are neglected and  $p_\theta = 0$ .

Distribution functions  $f_{e,i}(r, z, p_r, p_z, p_\theta)$  satisfy the steady-state Vlasov equation

$$\frac{d}{dt} f_{e,i} = 0 \quad (3)$$

solved with  $A_\theta^s, \phi^s$  self-consistently calculated from the equations

$$\frac{\partial}{\partial r} (r \frac{\partial}{\partial r} (r A_\theta^s)) + \frac{\partial}{\partial z} (A_\theta^s) = \frac{4\pi}{c} j_\theta \quad (4)$$

$$+ \frac{\partial}{\partial r} (r \frac{\partial}{\partial r} \phi^s) + \frac{\partial}{\partial z} \phi^s = 4\pi e (n_e - n_i) \quad \text{with}$$

$$n_{e,i} = (2\pi r)^2 / (d^3 p) f_{e,i} \quad \text{and } j_\theta = e n_e v_\theta = \int d^3 p v_\theta f_e \quad (5)$$

Hence we obtain two coupled nonlinear integro-differential equations

$$L^* A_\theta^s = J(A_\theta^s, \phi^s), \quad L \phi^s = Q(\phi^s, A_\theta^s) \quad (4^+)$$

with appropriate boundary conditions to be imposed at infinity or on finite conductors.

II. Exact Stationary Distribution Functions

To determine the  $f_{e,i}$  a knowledge of constants of motion is most useful since an arbitrary (differentiable) function of them solves (3). In the stationary case the total energy  $H_{e,i}$  and, for electrons,  $p_\theta$  are constants that allow for a class of exact solutions of (3) which can be written as

$$f_e = f_{e1}(H_e) g(p_\theta) \quad (5)$$

$$f_i = f_i(H_i) \quad (6)$$

where  $g(p_\theta)$  prescribes the momentum spread of the electrons, and  $f_{e1}$  is typically Gaussian-like for an ER, in contrast with other papers<sup>7,11</sup> where a  $\delta$ -function leading to a uniform density inside a sharp boundary was chosen.

Whether distribution functions (5), (6) are sufficiently general for an ER is a question of basic importance. In fact, it seems impossible in general to give explicitly an additional exact constant of motion comparable to the energy. Certain approximations are possible, however, which can be discussed more transparently in a model where transverse ( $r, z$ ) and longitudinal ( $\theta$ ) energies are decoupled.

III. Decoupling of Transverse and Longitudinal Energies

For a given value of  $p_\theta$  an equilibrium radius  $R(p_\theta)$  and corresponding minimum energy  $E_{e,\min}(p_\theta)$  are given for electrons according to the

<sup>+</sup>This work was performed under the terms of the agreement on association between the Max Planck Institut für Plasmaphysik and EURATOM

following variational principle:

$$\delta (H_e(r, z, p_x, p_z, p_\theta)) = 0 \quad (7)$$

Since in ER applications the "transverse" energy  $E_e - E_{\min}$  is nonrelativistic, we may expand the square root in (1) to obtain a transverse Hamiltonian  $H_{e\perp}$  with nonrelativistic features. We define a zero-order (i.e. neglecting self-fields) equilibrium radius  $R_0$  and minimum energy  $E_{\min}$ , for which we obtain from (7) (for  $B^{\text{ext}}$  symmetric in  $z$ ):

$$\frac{\partial}{\partial r} p_r^2 = 2p_r^2 \left( -B^{\text{ext}}_r + \frac{c}{R} \frac{\partial}{\partial R} p_r^2 \right) = 0, \quad E_{\min} = \left( \frac{m_0 c^2}{R_0} + \frac{c^2}{R_0} p_r^2 A_0(R_0) \right)^{1/2}$$

The desired expansion to first order is

$$H_e = \left( \frac{m_0 c^2}{R_0} + \frac{c^2}{R_0} p_r^2 \right)^{1/2} - \frac{c}{R_0} \frac{\partial}{\partial R} p_r^2$$

$$= \frac{m_0 c^2}{R_0} \left( 1 + \frac{p_r^2}{m_0 c^2} \right)^{1/2} - \frac{c}{R_0} \frac{\partial}{\partial R} \left( \frac{p_r^2}{m_0 c^2} \right)^{1/2}$$

with  $\frac{\partial}{\partial R} p_r^2 = E_{\min} \frac{\partial}{\partial R} \frac{p_r^2}{m_0 c^2}$ ,  $V_0 = p_r^2 / m_0 c^2$ ,  $p_r^2 = p_r^2 + \frac{c}{R_0} \frac{\partial}{\partial R} p_r^2$  and  $V_0 = 1 - \frac{1}{R_0^2}$  where it is assumed that higher variations of  $p_r^2$  than second order are negligible compared with self-field variations. Thus, we find with  $n = -R_0 \frac{\partial}{\partial R} \frac{p_r^2}{m_0 c^2}$ ,  $x = \frac{p_r^2}{m_0 c^2}$ ,  $z = \frac{p_z^2}{m_0 c^2}$ ,

$$H_{e\perp} = \frac{p_r^2 + p_z^2}{2m_0 c^2} + \frac{m_0 c^2 V_0}{2R_0^2} (1 - n) x^2 + n z^2 + \frac{c}{c} V_0 A_0(R_0) - \frac{c}{R_0} \frac{\partial}{\partial R} p_r^2 \quad (8)$$

#### IV. Approximate Solutions for Distribution Functions of a More General Nature

The exact solutions (5), (6) expressed in  $H_{e\perp}$ ,  $H_i$  prescribe densities in  $(x, p_x, z, p_z)$ -phase space uniform on surfaces of constant energy. Let us consider an ensemble of phase points uniformly distributed on the surface  $H = E_0$ . Let us now assume a change in the external field  $B^{\text{ext}}$  which deforms the energy surface. Clearly, a rapid change in  $B^{\text{ext}}$  may lead to nonstationary phase space flow. The considered ensemble then lies in general on a fluctuating surface different from any energy surface. Filamentation may lead after sufficiently long time to an effective stationary phase space distribution, which one can determine in general only by following the particle trajectories.

Next, let us consider a change  $B(\omega) \rightarrow B^{\text{ext}}$  which is slow ( $\tau$  the slowly varying time) compared with the short oscillation times of the system such that the instantaneous distribution is free from short-time fluctuations. Two situations are of interest at the time  $\tau$

(I): the original ensemble  $H(\omega) = E(\omega)$  is transformed into a new ensemble uniform on  $H(\tau) = E(\tau)$  with  $H(\tau)$  the new Hamiltonian

(II): (I) is not true

In case (I) typically ergodic behaviour is present. More recent works on ergodic theory<sup>12, 13, 14</sup> and computer calculations for two-dimensional particle motion<sup>15</sup> have shown that even in quite general situations - depending on the amount of coupling between different degrees of freedom - an energy surface is separated into invariant tori with Lebesgue measure greater than zero. There exist distribution functions nonuniform on energy surfaces. To determine them, one needs the additional invariants of the motion. Such invariants can in general be represented only in terms of asymptotic series, which were introduced in theories on adiabatic invariants relevant for confinement of particles in magnetic fields<sup>16, 17</sup>. (A simple exception is rotational symmetry in  $x, z$  which shall be excluded here.) With increasing (nonlinear) coupling in  $x, z$  computer calculations<sup>15</sup> have shown that "stochastic" trajectories which wander all over the whole energy

surface dominate over the ordered motion (confined to invariant sections). In this case the usual asymptotic series expansions for invariants cannot be applied. There is pronounced ergodic behaviour and case (I) appears to give the appropriate prescription of the phase space flow.

A rough estimate of the amount of nonlinear  $x, z$ -coupling in particle motion in realistic electron rings (with collective field strengths within the present limits) justifies the following treatment: 1) ions are described according to (I) with distribution functions (6) uniform on energy surfaces; 2) electron motion is weakly coupled and depends on still another invariant. The detailed form of the distribution functions will be established in the next section.

#### C. Adiabatically Changing Equilibria

Compression, ion loading and acceleration may be treated as slow processes compared with oscillation times of electrons and ions. The time-dependence of  $f_e, f_i$  during such adiabatic changes described by the parameter  $\tau$  can be established by using adiabatic invariants in accordance with the conclusions at the end of B IV.

##### I. The Ion Distribution Function

According to (I) ions on a surface  $H_i(\omega) = E(\omega)$  are redistributed on a new surface of  $H_i(\tau)$ . Because of Liouville's theorem the 4-dimensional phase space volume

$$I(E, \tau) = \int d\mathbf{p}_x d\mathbf{p}_z dx dz, \quad \frac{dI}{d\tau} = 0 \quad (9)$$

is invariant and permits us to determine  $E(\tau)$ . Hence we obtain an (adiabatically) invariant distribution function for ions (for constant ion number)

$$F_i(I) dI \equiv F_i(I(H_i, \tau)) dI \quad (10)$$

which is related to (6) according to

$$F_i(I) dI = \int f_i \frac{dE}{dI} dI \quad (10')$$

From (6) we obtain for  $H_i = \frac{p_r^2 + p_z^2}{2m_i} + V_i(x, z, \tau)$

$$I(E, \tau) = 2m_i \tau \int (E - V_i(\tau)) dx dz \quad (9')$$

and

$$m_i(x, z) dx dz = 2m_i \tau \int F_i(I(T + V_i, \tau)) dI$$

For rest-gas ionization ions are produced with zero kinetic energy (neglecting their small azimuthal velocity) in the potential trough built up by the instantaneous electric space charge. The ionization probability is proportional to the electron density; the ionization rate  $\alpha_i$  may be time-dependent. Hence we obtain the following differential change of the distribution function

$$\frac{\partial F_i(I, \tau)}{\partial t} dI = \alpha_i(t) \int m_e(x, z, t) dx dz \quad (11)$$

The integral can be transformed into a line integral along equipotential lines of  $V_i$

The functional determinant for transformation into curvilinear coordinates  $V_i, \sigma$  is derived as  $\frac{\partial(x, z)}{\partial(V_i, \sigma)} = |\nabla V_i|$  and with  $\frac{dV_i}{d\sigma} = \frac{d}{d\sigma} \frac{dI}{dI}$  we find

$$\frac{\partial F_i(I, \tau)}{\partial t} dI = \alpha_i(t) \frac{\partial E(I, \tau)}{\partial I} \int \frac{m_e(x, z, t) d\sigma}{|\nabla V_i|} \quad (11')$$

##### II. The Electron Distribution Function

To determine an invariant distribution function for electrons, we require two adiabatic invariants

riants instead of one for the ions. Taking into account nonlinear  $x, z$ -coupling, asymptotic series for the invariants should be the only correct procedure, but this is not useful for a straightforward numerical code. We therefore neglect  $x, z$ -coupling and obtain the simple separate adiabatic invariants

$$I_x(E_x, z) \equiv \int_{H_x \leq E_x} dP_x dz, \quad I_z(E_z, z) \equiv \int_{H_z \leq E_z} dP_z dz \quad (12)$$

with  $H_{x,z}(P_x, P_z, x, z, z) = H_x(P_x, x, z) + H_z(P_z, z, z)$

A better approximation could be obtained by using the scaling law for radial and axial betatron oscillations:  $\kappa_{x,z} \gg 1$ , which is valid for the present experiments. In this case the radial phase space volume  $I_x$  is again an invariant. The second invariant follows from the  $z$ -motion averaged over rapid oscillations due to the coupling with  $x$ .

With (12) the invariant distribution function can be written as

$$F_{e1}(I_x, I_z) dI_x dI_z \equiv F_{e1}(I_x(H_x, z), I_z(H_z, z)) dI_x dI_z \quad (13)$$

and the density (apart from integration over  $P_\theta$ ) is  $n_e(x, z) dx dz = \int F_{e1}(I_x, I_z) dP_x dP_z$

### III. Polarization and Particle Loss During Acceleration

When an accelerating  $\vec{B}_\perp$  or  $\vec{E}_\perp$  field is applied, forces acting on ions and electrons tend to polarize the ring in the  $z$ -direction. For sufficiently high acceleration particles evaporate from the ring as a result of the decreasing axial focussing. This results in a truncation of the distribution function (10) or (13) at a limiting value of  $I$  or  $I_x$  corresponding to the energy where the potential has a pass.

For magnetic acceleration we have in a coordinate system moving with the ring

$$H_{\perp} \equiv H_{\perp} + (eV_{\theta}/c B_r^{\text{ext}} - m_0 \gamma_0 b) z = H_{\perp} + K' z \quad (14)$$

where nonrelativistic axial velocity is assumed. Force balance yields  $(eV_{\theta}/c - m_0 \gamma_0 b) N_e = m_i b N_i$  and thus  $K' = N_i/N_e \kappa$ ,  $b = eV_{\theta}/c B_r^{\text{ext}} / (m_i N_i/N_e + m_0 \gamma_0)$

### D. Iterative Solution of the Self-Consistency Problem by a Numerical Code

For given invariant distribution functions (10), (13) the integro-differential equations (4') assume the following form, using (9') and (12)

$$A_0^s = -\frac{2e}{c} \int dP_\theta g(P_\theta) V_{\theta 0} \int F_{e1}(I_x, I_z) dP_x dP_z \quad (4')$$

$$L \phi^s = \frac{2e}{c} \int dP_\theta g(P_\theta) \int F_{e1}(I_x, I_z) dP_x dP_z - 8\pi m_i \int F_i(I) dI \quad (4'')$$

Self-consistent solutions for  $A_0^s, \phi^s$  are supposed to exist for physical reasons. Equations (4'') have to be solved taking into account possible truncation of  $F$  if there is insufficient focussing. Convergence of an iteration scheme to solve (4'') depends critically on the mathematical properties of the operator defining the iteration, i.e. its eigenvalue spectrum. The following physical quantities are expected to influence convergence: number of particles to be confined, attractive or repulsive self-forces, several particle species interacting with each other, variable total particle numbers, boundary conditions. As far as the author knows, no mathematical criteria are available concerning convergence of an appropriate iteration scheme for the present coupled equations problem.

The simplest "direct" iteration was attempted in the numerical code. In most of the cases it was convergent after few ( $\leq 5$ ) iteration cycles. When iteration failed relaxation was introduced which connects subsequent iteratives according to  $\psi^{(n+1)} = (1-\alpha)\psi^{(n)} + \alpha \psi^{(n+1)}$  ( $0 < \alpha \leq 1$ ). This "first-order relaxation" is convenient if direct iteratives oscillate about some solution.

In the present code divergence of both methods was used to indicate the nonexistence of an equilibrium solution. This is important for defining the maximum admissible accelerating force (holding power).

The numerical code has the following characteristics (details see<sup>18</sup>):

- 1) Toroidal geometry with an infinite conductivity boundary of rectangular cross-section to solve the Poisson and vector potential equations (on a 128 x 128 grid). Different electric and magnetic boundaries were allowed for to simulate a squirrel cage, which is transparent to magnetic fields<sup>19,20</sup>.

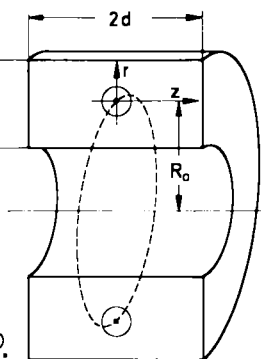


Fig.1 Geometry

- 2) After each step of differential ion production  $\Delta F_i = \frac{dF_i}{dt} dt$  (11') self-consistency is re-established according to (4').
- 3) At different stages of a full compression cycle, ion loading cycle and acceleration cycle the contribution of instabilities may be taken into account by increasing the occupied phase volumes (9), (12).

### E. Results

Computer runs are presented here with data adapted to the Garching ERA experiment (compressed rings):  $N_e = 5 \cdot 10^{12}$ ,  $R_0 = 2.3$  cm,  $\gamma_0 = 27.2$ ,  $n = 0.021$  (at the end of compression); no momentum spread for simplicity.

The electron distribution function was chosen as  $F_{e1} \sim \exp(-I_x/\mu + I_z/I_{\max}) \cdot \Theta(I_x/\mu + I_z - I_{\max})$ , with  $\Theta$  the step function and  $\mu = 6$  to obtain nearly circular ER cross-sections (small semi-axes  $a \approx b \approx 0.3$  cm).

These initial conditions are common to all examples listed below. The ring is then loaded with ions ( $f = N_i/N_e$ ,  $0 < f \leq 0.05$ ) and afterwards studied in two different surrounding structures (with acceleration):

- a) boundary CYL; two cylinders at  $r_{\perp} = R_0 \pm 1.25$  cm closed axially at  $z = \pm 2.5$  cm (already present before ion loading)
- b) boundary SQC; cylinder at  $r_{\perp} = R_0 - 1.25$ ; electric image cylinder at  $r_{\perp e} = R_0/P_{\text{sqc}}$  ( $0.6 \leq P_{\text{sqc}} \leq 0.8$ ), magnetic image cylinder at  $r_{\perp m} = R_0 + 3(r_{\perp e} - R_0)$ .  $P_{\text{sqc}}$  is a measure of the focussing strength of the "squirrel cage" simulated hereby.

Table 1 shows characteristic ring data for the unloaded ER and loaded rings in CYL and SQC

(for  $n = 0$ , no accel.).  $2\bar{a}$ ,  $2\bar{b}$  axial and radial electron ring width at half maximum density;  $eE_{z\text{peak}}$ ,  $eE_{z\text{edge ions}}$  peak electric field and the electric field at the edge of the ion subring that are produced by electron space charge;  $\Delta_e v_z^2$  self-field contribution to squared axial tune of the electrons (including toroidal and image effects);  $N_e/N_{e0}$  confined electrons as fraction of originally ( $n=0$ ) present electrons.

### Conclusion

#### 1) Inhomogeneous electron and ion densities.

Fig. 2-4 show that the half-width of the density profiles of the ions is a factor 2 smaller than that of the electrons.

#### 2) Toroidal effects.

In relativistic electron rings an axial defocussing force occurs<sup>5</sup> which is usually much stronger than the  $1/r^2$ -repulsion of straight beams. Table 1 shows that without a squirrel cage an  $f \gtrsim 0.5$  (Ex. ②) is necessary to keep all electrons confined (at  $n = 0$ , zero accel.).

#### 3) "Squirrel Cage" focussing.

With a SQC the electron contribution  $\Delta_e v_z^2$  can be made positive, which guarantees axial focussing of the electrons independent of the ion loading fraction ( $f$ ), provided that  $P_{\text{SQC}}$  is larger than 0.65 (Table 1).

#### 4) Acceleration and "holding power".

We define the maximum "holding power" here as the highest admissible accelerating force  $\kappa$  (acting on the ions, see (14)) at which at least a residue of ions remains trapped in the ring. On acceleration an electron-ion ring is polarized, as a result of which the axial focussing of either particle species is reduced.

Two principal situations can then be distinguished:

- Insufficient image focussing if the electron self-field contribution  $\Delta_e v_z^2$  is nearly zero or negative (for very small  $f$ ) as in ex. ②-④ and with the weak SQC in ex. ⑫, ⑬. In this case electrons are gradually lost from the ring with increasing acceleration until complete ring disintegration and spontaneous loss of all ions (Fig. 7). Without SQC nearly no acceleration is possible for  $f = 0.175$ . The maximum "holding power" is typically  $\leq 25\%$  of the peak electric field  $eE_{z\text{peak}}$ .
- Dominant image (SQC) focussing is present if  $\Delta_e v_z^2$  is sufficiently positive as in ex. ⑥-⑪, where electrons are well-focussed even for very small  $f$ . In this case ions are gradually lost from the ring above a threshold acceleration ( $\approx 7.5$  MeV/m). The maximum "holding power" is about 75% of  $eE_{z\text{peak}}$  (Fig. 7).

### Acknowledgements

The author is indebted to Prof. A. Schlüter and Dr. P. Merkel for discussions and to E. Springmann for computer programming.

### Bibliography

- J.P. Boris, R.Lee, NRL-Rep.2284(1971)
- W.H.Kegel, Plasma Physics 12, 105(1969)
- S.Yoshikawa, Princeton-MATT-816(1972)
- P.Merkel, MPI f. Plasmaphysik IPP 0/18 (1973)
- L.J.Laslett, LRL Berkeley, ERAN 30(1969)
- W.A.Perkins, LRL Berkeley, ERAN 97(1970)
- R.C.Davidson,J.D.Lawson, Univ.of Maryland-Rep.204PO29(1972)
- L.J.Laslett, Symp.on Electr.Ring Accel.ERA19
- C.Bovet, LRL Berkeley, ERAN 88 (1970)
- A.A.Drozdovskii, Rep.ITEF-10, Moscow(1973)
- N.Y.Kazarinov, E.A.Perelshtein, Symp.on Coll. Meth.of Acceleration, Dubna(1972)
- V.I.Arnold, in V.I.Arnold a.A.Avez, Problèmes Ergodiques de la Mécan.Classique, Paris(1967)
- J.Moser, Nachr.Akad.Wiss.Göttingen 1,1(1962)
- A.N.Kolmogorov, in R.Abraham, Found.of Mechan. App.D, New York(1967)
- M.Hénon, C.Heiles, Astron.J.69, 73(1964)
- M.Kruskal, J.Math.Phys.3, 806(1962)
- B McNamara, K.J.Whiteman, J.Math.Phys.8, 2029 (1967)
- I.Hofmann, IPP 0/21 (1974)
- G.V.Dolbilov et.al., JINR-P9-4737, Dubna(1969)
- I.Hofmann, IPP 0/16 (1973)

### Figures

(list of examples see Table 1)

Fig.

- Electron density profiles, ex. ① (densities with maximum normalized to 1)
- Electron a.ion (dashed) dens.prof. ex. ②
- Electron a.ion (dashed) dens.prof. ex. ④
- Electron a.ion (dashed) dens.prof. ex. ⑧ ⑨
- Axial potent.f.electr.a.ions(dashed)ex. ② ④
- Axial potent.f.electr.a.ions(dashed)ex. ⑧ ⑩
- $N_e/N_{e0}$  or  $N_i/N_{i0}$  (fraction of confined particl. to originally-before roll out-pres.particl.) as function of accelerating force. The left-side curves show examples with prevalent electron loss ( $N_e/N_{e0} \rightarrow 0$ ; insufficient image focussing), the right-side curves prevalent ion loss ( $N_i/N_{i0} \rightarrow 0$ ; dominant image focussing). The hatched regions cover  $0.001 \leq f \leq 0.025$ . The dotted appendices indicate (numerical) ring disintegration.
- Density plots for electrons and ions in  $(x, z)$ -cross-sections, for ex. ③ ⑧, ⑨:
  - before ion loading ( $n=0.021$ ,  $R_0=2.3$  cm);
  - loaded ring at  $n=0.005$ ; accelerated rings. The plots show lines of constant density  $n_e(x, z)$  and  $n_i(x, z)$  with uniform level difference  $\Delta n$ . The ion subring is thinner than the electron ring and slightly shifted to smaller radius.

Table 1

	$f$	bound. [cm]	$\bar{a}$ [cm]	$\bar{b}$ [cm]	$eE_{z\text{peak}}$	$eE_{z\text{edge ions}}$ [MeV/m]	$\Delta_e v_z^2$	$N_e N_{e0}$
ex. ①	before ion loading $n=0.021$	32	.29	24		-	-.0067	1
ex. ②	.05	CYL	.23	.30	22	22	-.0069	.97
ex. ③	.025		.25	.30	15	15	-.0047	.66
ex. ④	.0475		.23	.31	12	9	-.0036	.51
ex. ⑤	.025	$P_{\text{SQC}}=8$	.25	.29	25	23	.026	1
ex. ⑦	.001		.29	.29	24	22	.025	1
ex. ⑧	.025	$P_{\text{SQC}}=7$	.30	.29	21	21	.0010	1
ex. ⑨	.001		.50	.29	17	17	.0021	1
ex. ⑩	.025	$P_{\text{SQC}}=55$	.31	.29	19	19	-.0018	1
ex. ⑪	.001		.70	.29	13	13	.002	1
ex. ⑫	.05	$P_{\text{SQC}}=6$	.20	.29	29	27	.0053	1

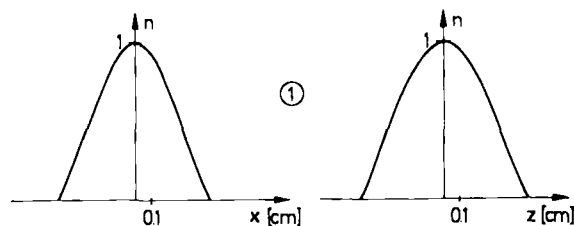


Fig. 1

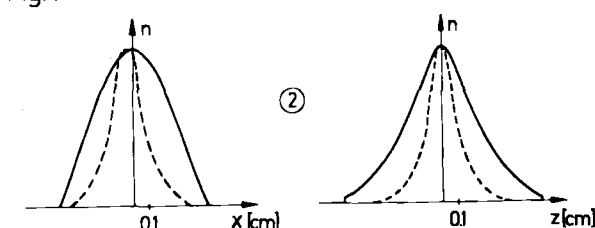


Fig. 2

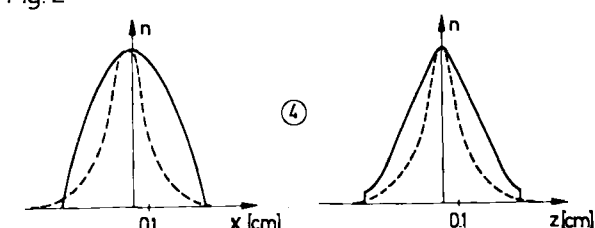


Fig. 3

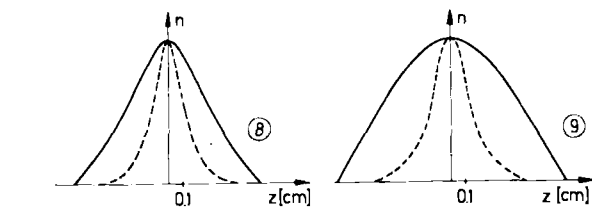


Fig. 4

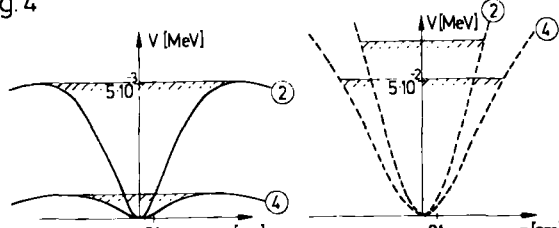


Fig. 5

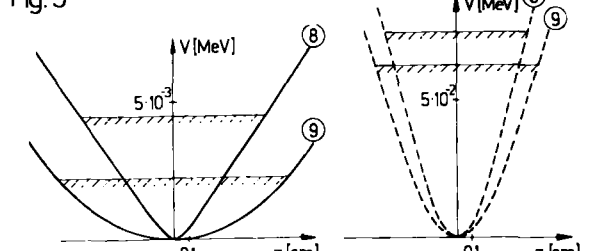


Fig. 6

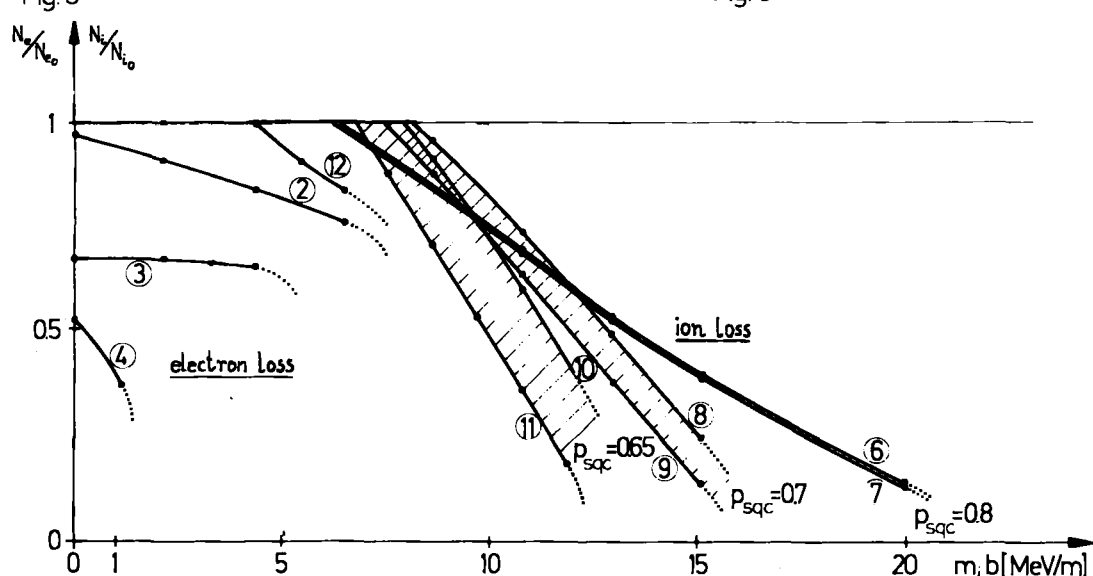


Fig. 7

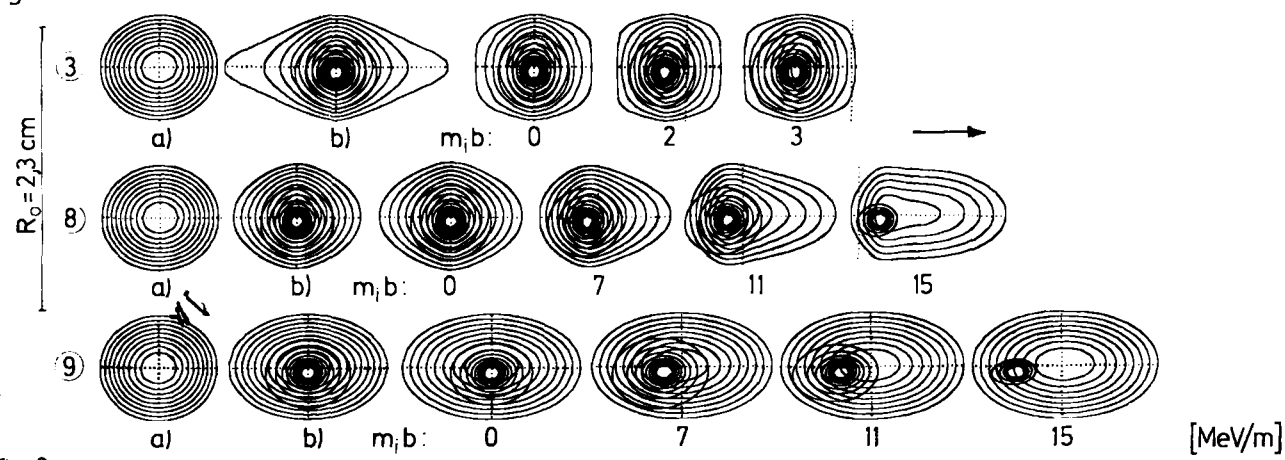


Fig. 8